BMC Cancer

RESEARCH

Open Access

Matrix stiffness-related extracellular matrix signatures and the DYNLL1 protein promote hepatocellular carcinoma progression through the Wnt/β-catenin pathway

Yang Shen[1†], Jiayu Chen[1†], Zhuolin Zhou[1†], Jingyu Wu[1], Xinyao Hu[1], Yangtao Xu[1], Jiayi Li[1], Ling Wang[1], Siyu Wang[1], Shuhong Yu[1], Ling Feng[1*] and Ximing Xu[1*]

Abstract

Background In hepatocellular carcinoma (HCC) treatment, first-line targeted therapy in combination with immune checkpoint inhibitors (ICIs) has improved patient prognosis, but the 5-year survival rate is far from satisfactory. Studies have shown that the extracellular matrix (ECM) is an essential part of the tumour microenvironment (TME) and participates in the progression of malignant tumours. ECM remodelling can enhance matrix stiffness in cirrhosis patients, induce an immunosuppressive microenvironment network, and affect the efficacy of targeted therapies and ICIs for treating HCC. However, the exact mechanism is still unclear.

Methods We downloaded data from public databases, selected differentially expressed ECM proteins associated with matrix stiffness, constructed and validated a prognostic model of HCC using Lasso Cox regression, and investigated the roles and mechanism of one of the ECM proteins, dynein light chain LC8-type 1 (DYNLL1), in HCC proliferation, migration, and apoptosis via in vitro experiments.

Results In this study, the risk score of the matrix stiffness-related ECM protein model effectively predicted the prognosis of HCC patients. The high- and low-risk subgroups of the model also showed differences in immune cells, immune functions, and drug sensitivity. DYNLL1 promoted HCC cell progression and migration and inhibited HCC cell apoptosis through the Wnt/β-catenin pathway in vitro.

Conclusion The expression of matrix stiffness-related ECM proteins could be an independent predictor of HCC prognosis. DYNLL1, an oncogenic gene in HCC, has the potential to be a new target for HCC treatment.

†Yang Shen, Jiayu Chen, Zhuolin Zhou these authors contributed equally to this work.

*Correspondence:
Ling Feng
1262168646@qq.com
Ximing Xu
doctorxu120@aliyun.com

Full list of author information is available at the end of the article

Keywords Hepatocellular carcinoma, Matrix stiffness, Extracellular matrix proteins, Prognostic model, DYNLL1, Wnt/β-catenin pathway

Introduction

Hepatocellular carcinoma (HCC) is the second leading cause of malignant tumour-related mortality worldwide [1]. This is because once diagnosed, the majority of patients are at an intermediate to advanced stage and are at a greater risk of developing metastases to other sites, such as the lungs. Even after hepatectomy, recurrent intra- or extrahepatic metastases occur in 70% of patients within 5 years of surgery [2]. Therefore, it is crucial to uncover the underlying mechanisms driving accelerated tumour progression, which could help inhibit rapid cancer spread and provide more treatment options for HCC patients. However, the molecular mechanisms responsible for the dysregulation of tumour cell proliferation in HCC are currently unknown.

The extracellular matrix (ECM) is a sophisticated assembly of proteins, polysaccharides, and glycoproteins that serves as a dynamic framework offering structural integrity and biochemical assistance to cells and tissues [3]. High matrix stiffness is a reliable indicator of HCC occurrence and is associated with reduced survival in HCC patients [4]. Liver inflammation or injury disrupts the balance between the synthesis and degradation of ECM proteins, leading to excessive deposition and fibrosis of liver tissue, which can eventually progress to HCC [5–7]. As a crucial element of the tumour microenvironment (TME), the ECM facilitates tumour cell growth, metastasis, and chemoresistance through various mechanisms and may aid in the ability of cancer to evade immune recognition [8–10]. For instance, the matrix stiffness-related ECM protein TGF-β1 promotes tumour progression and immune evasion by inducing M2 polarization in tumour-associated macrophages (TAMs) [11, 12]. This finding underscores the potential of matrix stiffness-related ECM proteins as targets for antitumour immunotherapy. Thus, they represent an important area of research.

Dynein light chain LC8-type 1 (DYNLL1), a signature gene, is an essential constituent of the cytoplasmic dynamin complex and plays a pivotal role in cellular processes dependent on cytoskeletal reorganization [13]. Furthermore, DYNLL1 has been shown to participate in cancer progression and chemoresistance [14–16]. DYNLL1 was found to negatively regulate MRE11-mediated homologous recombination to reduce DNA repair by binding to MRE11, a component of the MRN complex with nuclease activity [16–18].Caglar Berkel. et al. [19] further found that in advanced or high-grade plasmacytoid ovarian cancer, the decreased expression of DYNLL1 along with its transcriptional activator ATMIN leads to an increase in MRE11-mediated double-stranded DNA break repair events thereby contributing to ovarian cancer being more aggressive, metastatic, and chemo-resistant. However, reports and studies on DYNLL1 in HCC patients are limited. Liu, et al. revealed that DYNLL1 can regulate the cell cycle in HCC through ILF2/CDK4 axis and promote palbociclib sensitivity [20]. No other experimental studies have been conducted to determine its specific contribution to HCC.

Therefore, in this study, we constructed a prognostic matrix stiffness-related ECM gene signature and analysed its clinical significance in HCC patients. We also explored the potential roles of DYNLL1 in the progression of HCC by investigating its relevant molecular mechanism in HCC in vitro to validate its function in HCC cells (Fig. 1). Our study may provide a new therapeutic target for treatment of HCC patients.

Materials and methods

Dataset source

The gene expression profiles were downloaded from The Cancer Genome Atlas (TCGA_LIHC) database (https://portal.gdc.cancer.gov/projects/TCGA-LIHC) and the International Cancer Genome Consortium (ICGC) database (https://dcc.icgc.org/releases/current/Projects/LIRI-JP). ECM gene lists were downloaded from the GeneCards database (https://www.genecards.org/).

Identification of differentially expressed genes (DEGs) associated with matrix stiffness We used the R package 'Limma' [21] to identify DEGs in the TCGA_LIHC cohort between the HCC and normal patient groups, and a false discovery rate (FDR) value<0.05 was used as cutoffs. Since the expression of lysyl oxidase (LOX) and collagen 1 alpha 1 chain (COL1A1) is responsive to matrix stiffness, we divided the patients from the TCGA into LOX and COL1A1 high-expression groups according to the median expression of the two genes, and defined genes high-expressed in the groups as high matrix stiffness-related genes. We finally intersected the DEGs with the high matrix stiffness-related genes, and the ECM-related genes to examine high matrix stiffness-related ECM DEGs.

Gene function enrichment analysis The R package 'ClusterProfiler' [22] was used to perform the gene function enrichment analysis based on the Kyoto Encyclopedia of Genes and Genomes (KEGG) comprehensive database.

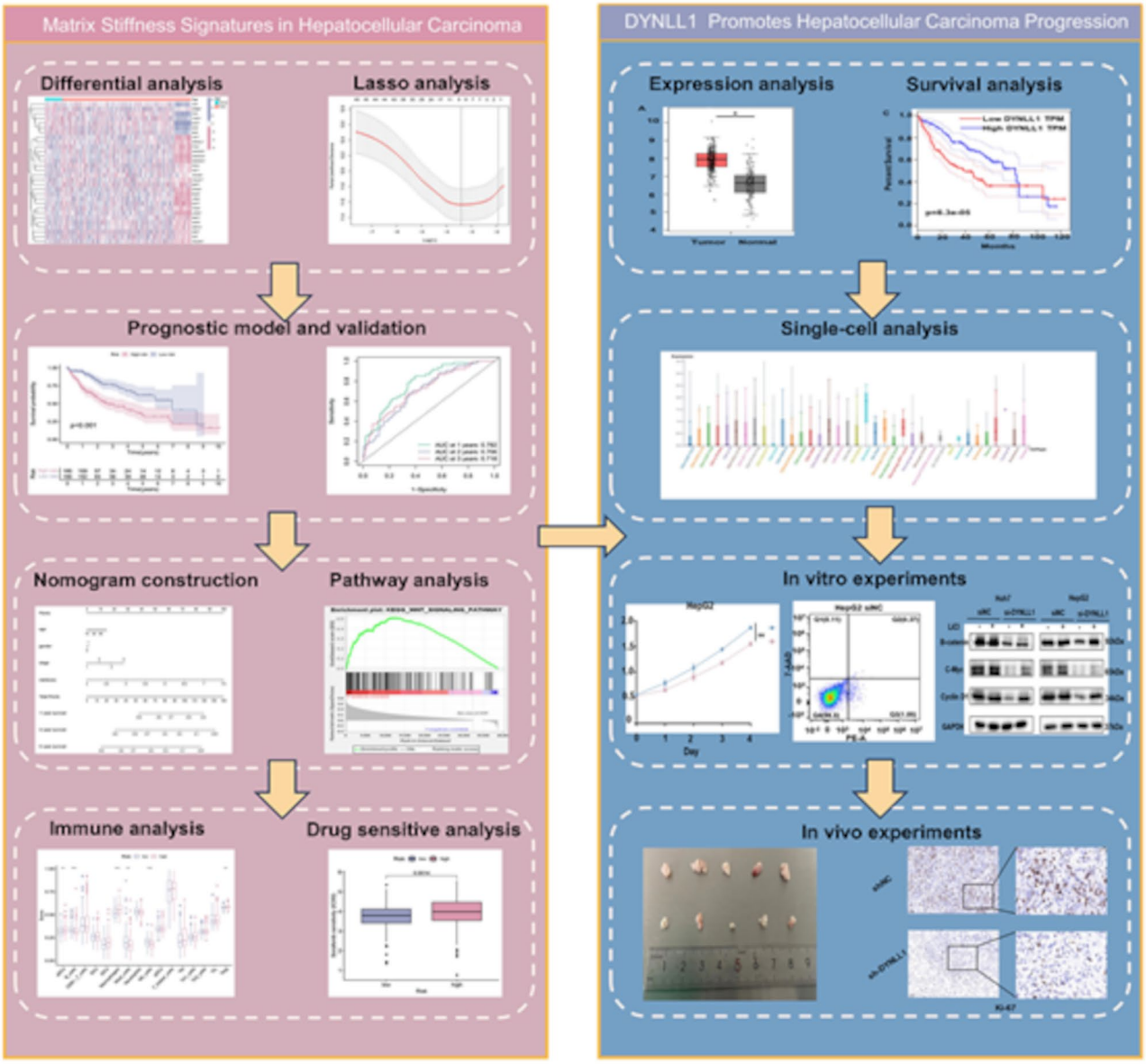

Fig. 1 Flowchart of the study

Mutation landscape analysis The R package 'maftools' [23] was used to extract and describe the mutation landscape of the TCGA cohort.

Construction and validation of the matrix stiffness-related ECM gene signature model The training cohort consisted of TCGA_LIHC datasets, while the validation cohort consisted of ICGC datasets. Lasso regression and univariate Cox analysis were used to screen the nine genes for which the model was constructed: MMP1, ECT2, DYNLL1, NCBP2, CTSA, TRAPPC4, EGLN3, and SRP72. The formula for calculating the risk score of the prognostic model was as follows:

$$\text{Risk score} = \sum_{n=1}^{i} Confidence\ (genei) \times Expression\ (genei).$$

Analysis of immunological properties The R packages 'GSVA' [24] and 'GSEABase' [25] were used to perform ssGSEA, which calculated the enrichment of 16 immune-related cell terms and 13 immune-related terms in HCC samples.

Sensitivity analysis of common drugs The evaluation of the sensitivity of common drugs was performed using the R package 'oncoPredict' [26].

Single-cell analysis The expression of DYNLL1 in several individual single HCC cells from different datasets was determined from the TISCH2 database (http://tisch.comp-genomics.org/). Single-cell data were acquired from the scTIME portal (sctime.sklehabc.com), and UMAP analysis was also performed on the website.

Immunohistochemistry (IHC) staining The tissues were first dewaxed, hydrated, and subjected to antigen retrieval. Then, 3% hydrogen peroxide was used to inhibit endogenous peroxidase activity for 15 min, and BSA was used to block the sections. Next, the samples were incubated with a primary antibody overnight at 4 °C and then with a secondary antibody for 50 min. Then, we developed the colour with DAB, restained the sections with haematoxylin, and finally dehydrated and sealed the samples. Images were acquired by microscopy and quantified using ImageJ software (National Institute of Health, Bethesda, MD, USA).

Cell culture The human HCC cell lines Huh7 and HepG2 (purchased from Procell Life Science & Technology Co., Ltd., Wuhan, China) were cultured in high-glucose Dulbecco's modified Eagle's medium (DMEM) supplemented with 1% antibiotics and 10% foetal bovine serum (FBS; Thermo Fisher Scientific, Inc., Waltham, MA, USA). The cells were cultured in a humidified incubator at 37 °C containing 5% CO_2.

Cell transfection The siRNAs targeting DYNLL1 were purchased from Suzhou GenePharma Co., Ltd. The sequences of the siRNAs used were as follows: si-1, ACCAAACACUUCAUCUACUUCTT; si-2, UGGCCAUUCUUCUGUUCAAAUTT; and si-3, ACAAGGACUGCAGCCUAAAUUTT. Transient transfection was performed using Lipofectamine 6000 (Beyotime Biotechnology, Shanghai, China). The cells were seeded at 6×10^4 cells/well in 6-well plates for 24 h, and when the cell density was 50-70%, the cells were transfected with siRNAs for 48 h for real-time quantitative PCR or 72 h for Western blotting analysis to determine the transfection efficacy. The sequence with the best interference was selected for the subsequent experiments.

Real-time quantitative PCR (qRT–PCR) Total RNA was extracted using TRIzol reagent (Servicebio, Wuhan, China) and reverse transcribed using a SweScript RT II First Strand cDNA Synthesis Kit (Servicebio). The obtained cDNA was amplified using 2×Universal Blue SYBR Green qPCR Master Mix (Servicebio). The $2^{-\triangle\triangle CT}$ method was used to calculate the relative expression of genes. The primers used for DYNLL1 were as follows: forward primer, AGAGATGCAACAGGACTCGGT; reverse primer, CCAGGTGGGATTGTACTTCTTG. The primers for GAPDH were as follows: forward primer, AATCAGAGTACATGCGACTGAGA; reverse primer, GCTGTATCCTTCGCTGTTTCC.

Western blotting All procedures were performed on ice. First, the samples were washed three times with precooled PBS and filtered dry. Next, the samples were treated with RIPA lysis buffer containing 1% phosphatase inhibitors for 15–20 min. Then, the samples were collected, further disrupted with a sonicator and centrifuged at 12,000 rpm for 15 min. Finally, the supernatant was collected, mixed with 1/4 volume of 5× loading buffer, boiled at 100 °C for 5 min and stored at -20 °C. Proteins were concentrated and separated using a 10% SDS polyacrylamide gel at 80 V for the concentration gel and 120 V for the separation gel and then transferred to a PVDF membrane (Millipore, NJ, USA) at 200 mA. The membranes were blocked with rapid sealing solution (Servicebio) for 10–30 min at room temperature and incubated with the corresponding primary antibodies overnight at 4 °C. The membranes were then incubated with anti-rabbit or anti-mouse horseradish peroxidase (HRP)-labelled secondary antibodies for 1 h at room temperature, after which the bands were visualized using a chemiluminescence kit (Servicebio). The primary antibodies used are listed in Table S1.

Cell proliferation assay The transfected cells were seeded into 96-well plates for culture at 8000 cells/well, and 10 µl of CCK-8 reagent (Servicebio) was added to the wells at 0 h, 24 h, 48 h, 72 h, and 96 h to incubate with the cells in the dark for 1 h 45 min, after which the OD at 450 nm was measured on an enzyme labeller (ELx800 Microplate Reader, BioTek Instruments, Winooski, VT, USA).

Wound healing assay The transfected cells were seeded into 6-well plates at a density of 3×10^5 cells/well, and when the cells were fully confluent, a wound was drawn perpendicular to the 6-well plate with a 200 µL lance tip. Gap closure was monitored under a microscope and digital camera (CK30-SLP; Olympus, Tokyo, Japan) at 0 h, 24 h, 48 h, and 72 h. Images were analysed using ImageJ software (National Institute of Health, Bethesda, MD, USA).

Flow cytometry Apoptosis was detected using an annexin V-phycoerythrin (PE)/7-aminoactinomycin D (7-AAD) kit (Servicebio). The cells were washed with cold PBS three times and resuspended in 100 µL of 1× binding buffer. Then, the cells were stained with 5 µL of 7-AAD and 5 µL of annexin V-PE and incubated in the dark for 15–30 min. Finally, 400 µL of binding buffer was added, and apoptosis was detected using a Beckman cytoFLEX flow cytometer (Beckman Coulter, CA, USA) and anal-

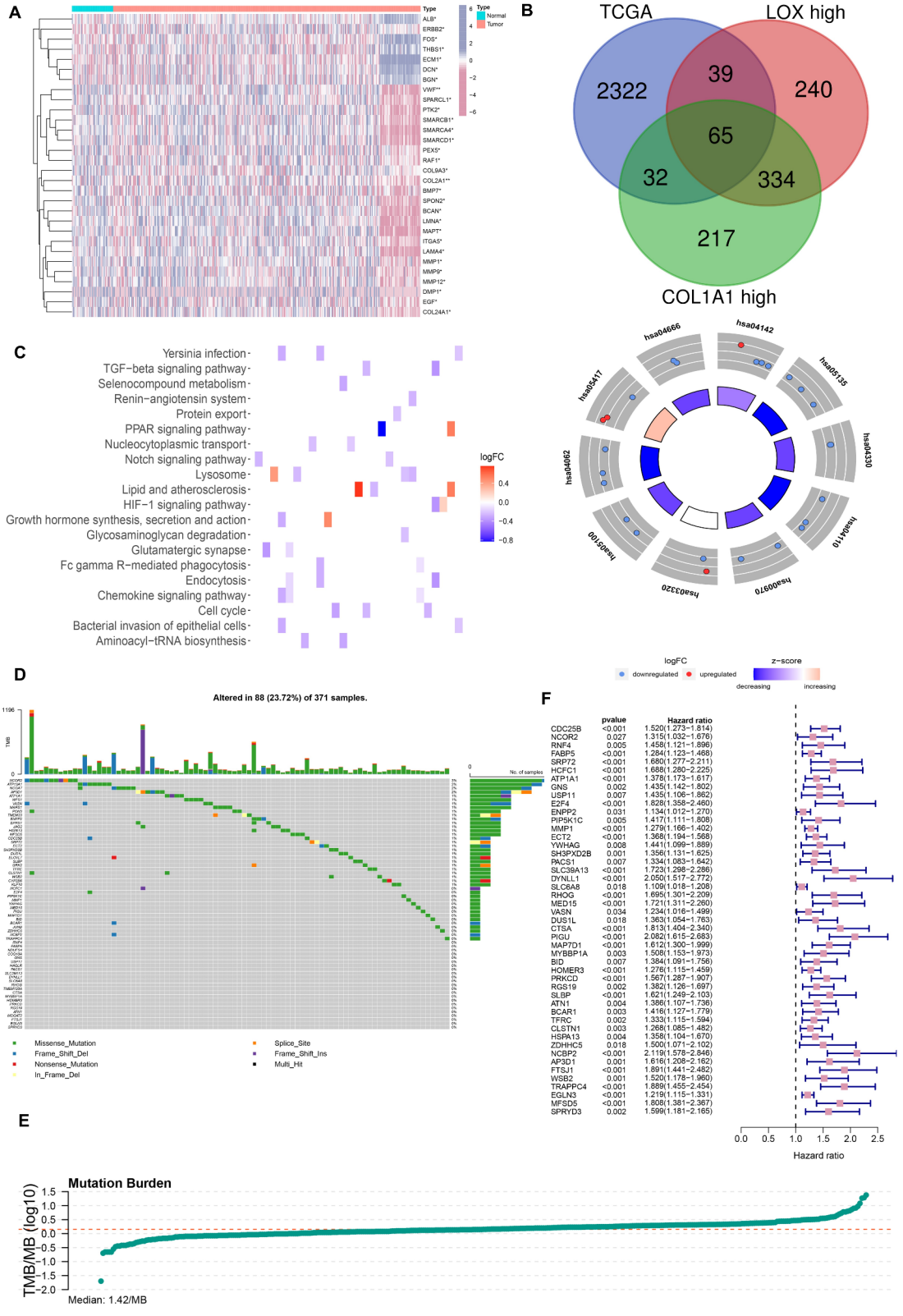

Fig. 2 (See legend on next page.)

(See figure on previous page.)

Fig. 2 Identification of the matrix stiffness-related ECM genes with prognostic significance in HCC. **(A)** Identification of the top 30 DEGs for HCC in the TCGA database. **(B)** Venn diagram showing 65 matrix stiffness-related ECM-related genes. **(C-D)** Heatmap and circle plot of KEGG analysis of matrix stiffness-related ECM genes; hsa04142, lysosome; hsa05135, *Yersinia* infection; hsa04330, Notch signalling pathway; hsa04110, cell cycle; hsa00970, aminoacyl-tRNA biosynthesis; hsa03320, PPAR signalling pathway; hsa05100, bacterial invasion of epithelial cells; hsa04062, chemokine signalling pathway; hsa05417, lipid and atherosclerosis; and hsa04666, Fc gamma R-mediated phagocytosis. **(D)** Mutational landscape of matrix stiffness-related ECM genes in the TCGA cohort. **(E)** The median TMB of matrix stiffness-related ECM genes. **(F)** Forest plot of univariate Cox regression analysis for matrix stiffness-related ECM genes with significant prognostic value

ysed using FlowJo™ v10 Software (BD Life Sciences, NJ, USA).

Xenograft nude mouse model Stable DYNLL1 knockdown huh7 cells were constructed by transfecting the huh7 cells with specific lentivirus (Suzhou GenePharma Co., Ltd.), then the transfected cells were added with 1.5 ug/ml puromycin and maintained for 1 week. Two groups of 5-week-old BALB/c nude mice were randomly selected. The nude mice were anesthetized with 2% isoflurane by inhalation and injected subcutaneously with the stable DYNLL1 knockdown huh7 cells. Tumour volumes ($V = \text{length} \times \text{width}^2 \times 0.5$) were measured every 3 days. The mice were euthanized by intraperitoneal injection of 100 mg/kg pentobarbital, and the tumours were excised and weighed after 15 days. All animals received humane care according to NIH (USA) guidelines. The study related to animals was approved by the Ethics Committee of Renmin Hospital of Wuhan University (202300384) on Jan 1, 2024.

Statistical analysis Student's t test or the Wilcoxon test was used to analyse continuous data. Statistical analysis was performed using GraphPad Prism 8.0 (GraphPad Software Inc., San Diego, CA, USA) and R version 4.2.1 (version 4.2.1, https://www.r-project.org/ [27]).

Results

Identification of matrix stiffness-related ECM genes in HCC

We downloaded the gene expression data from the TCGA database and screened 2458 DEGs, and the top 30 DEGs are shown in Fig. 2A. Considering that the expression levels of LOX and COL1A1 correlate with matrix stiffness [28, 29], we divided HCC patients from TCGA into LOX and COL1A1 high-expression groups according to the median expression of the genes LOX and COL1A1, respectively. We then examined the intersection of DEGs from HCC patients with high expression of both LOX and COL1A1 to determine which DEGs were most likely correlated with high matrix stiffness (Fig. 2B). Finally, 65 matrix stiffness-related ECM genes were chosen for further analysis (Fig. 2B). We then performed KEGG pathway enrichment analysis and found that the genes we obtained were positively correlated with the lysosome pathway and negatively correlated with the notch signalling pathway, the cell cycle, the PPAR signalling pathway, chemokine signalling pathways, the TGF-beta signalling pathway and the HIF-1 signalling pathway (Fig. 2C, D).

Mutation analysis of the matrix stiffness-related ECM genes and construction of the prognostic signature

Subsequently, we performed somatic mutation analysis to reveal the relationship between matrix stiffness-related ECM genes and mutations. We found that the NCOR2 gene had the highest mutation rate (3%), followed by three genes (ATP13A1, NCOA7, AND AP3D1), with a mutation rate of 2% (Fig. 2D). The median tumour mutation burden (TMB) of these genes was 1.42 mutations/MB (Fig. 2E). To construct the prognostic signature, we obtained the clinical data of HCC patients from TCGA and used univariate Cox regression to analyse the expression of DEGs for Hazard ratio (HR) and p values associated with survival, and 47 genes with p values < 0.05, which were associated with survival in HCC patients, were ultimately screened for further analysis (Fig. 2F).

The potential of the matrix stiffness-related ECM gene signature to predict the prognosis of HCC patients

The TCGA_LIHC dataset was used as the training cohort, and the ICGC LRIR_JP dataset was used as the testing cohort. Finally, nine genes (MMP1, ECT2, DYNLL1, NCBP2, CTSA, PIGU, TRAPPC4, EGLN3, and SRP72) for constructing the signature were obtained by Lasso regression analysis (Fig. 3A, B). A risk score was generated based on the expression of these nine genes, and patients were categorized into high- and low-risk groups according to their risk scores. Survival analysis revealed that patients in the high-risk group had a poorer prognosis (Fig. 3C, $p < 0.001$), and the same results were obtained using the ICGC dataset as the validation cohort (Fig. 3D, $p < 0.001$), which further validated the prognostic potential of our signature. According to the ROC curves, the AUCs of the signatures for predicting 1-, 2- and 3-year overall survival (OS) were 0.782, 0.706, and 0.718, respectively, in the TCGA cohort (Fig. 3E) and 0.757, 0.644, and 0.622, respectively, in the ICGC cohort (Fig. 3F). The risk score plot showed that patients in both the training and testing cohorts could be divided into two groups according to the risk score (Fig. 3G, H). Survival status distribution plots showed that in both the TCGA (Fig. 3I) and ICGC data (Fig. 3J), as the risk score increased, patient mortality increased, and survival time decreased. Subsequently, the PCA (Fig. 3K, L) and t-SNE

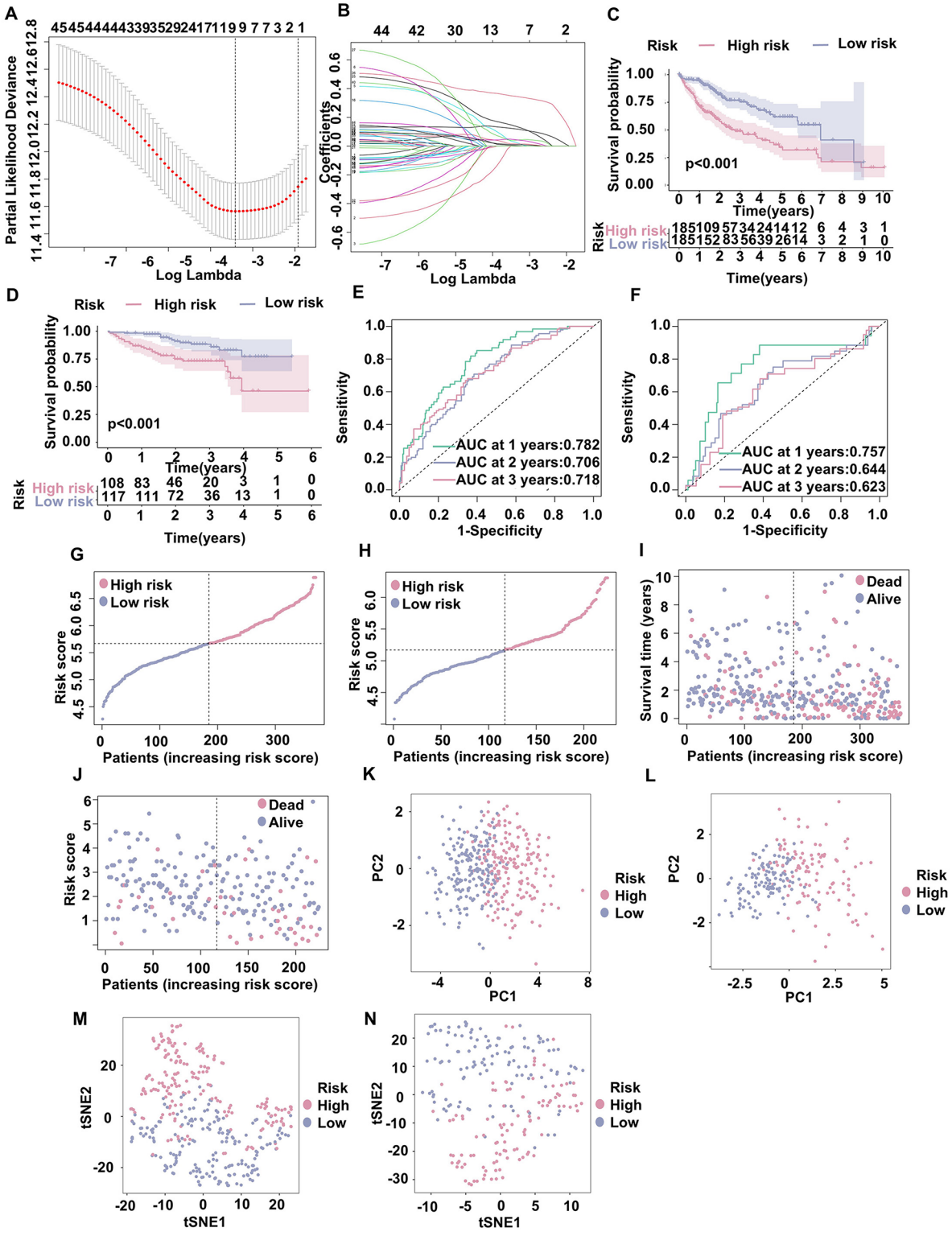

Fig. 3 The prognostic signature of the risk score analyses for the nine matrix stiffness-related ECM genes. (**A**) The optimal turning parameters (log λ) were selected using tenfold cross-validation. (**B**) Construction of a Lasso regression model. (**C**-**D**) Kaplan–Meier analysis of the OS rate of HCC patients in the high- and low-risk groups in the training and testing cohorts. (**E**-**F**) The ROC curves of the training and testing cohorts for overall survival at 1 year, 2 years, and 3 years. (**G**-**H**) Distribution of risk scores of the matrix stiffness-related ECM gene model in the training and testing cohorts. (**I**-**J**) Overall survival state distributions for the training and testing cohorts. (**K**-**L**) Principal component analysis (PCA) between the high- and low-risk groups in the training and testing cohorts. (**M**-**N**) T-distributed stochastic neighbour embedding (t-SNE) between the high- and low-risk groups in the training and testing cohorts

(Fig. 3M, N) maps were used to visualize the ability of the prognostic signature to identify HCC patients in both the TCGA and ICGC databases.

We then conducted univariate and multivariate independent prognostic analyses to measure the independent prognostic value of the gene signature. In the TCGA cohort, univariate analysis revealed that both the stage and risk score were significantly correlated with overall survival time ($p<0.001$), and the HR for the risk score was 3.548 (Fig. 4A). In addition, multivariate analysis confirmed the independent prognostic potential of the gene signature, with an HR of 2.886 (Fig. 4C, $p<0.001$). In the ICGC cohort, univariate and multivariate independent prognostic analyses also indicated that the signature was a credible independent prognostic factor for OS in HCC patients (Fig. 4B, HR=2.973, $p<0.001$; Fig. 4D, HR=2.167, $p<0.001$). A heatmap of the relationship between the risk score and clinical significance is shown in Fig. 4E. Furthermore, we constructed nomogram maps to predict 1-, 3-, and 5-year survival in patients with HCC using age, sex, stage, and risk score (Fig. 5A). A high score indicated poor clinical outcomes. The calibration plots were used to assess the accuracy of the nomogram model (Fig. 5B, C, D, E). Collectively, these data show that the matrix stiffness-related ECM gene signature had a good correlation with clinical prognosis and could independently predict the prognosis of HCC patients.

Pathway analysis and immune infiltration

GSEA showed that the genes involved in the signature were involved mainly in tumour and immune response-related signalling pathways, such as the Notch signalling pathway, MAPK signalling pathway, WNT signalling pathway, T-cell receptor signalling pathway, and natural killer cell-mediated cytotoxicity (Supplementary Figure S1). We quantified the enrichment scores of ssGSEA for different immune cell subgroups and immune-related pathways to further explore the correlation between risk scores and immune cells and function. The results showed that in both the TCGA and ICGC cohorts, B cells and NK cells were more abundant in the low-risk group, while macrophages were more abundant in the high-risk group (Fig. 6A, B). The immune function scores of the type I IFN response and type II IFN response were greater in the low-risk group (Fig. 6C, D). Moreover, the expression levels of CD86 (Fig. 6E), CD274 (Fig. 6F), CTLA4 (Fig. 6G), FAP (Fig. 6H), FOXP5 (Fig. 6I), IDO1 (Fig. 6J), IL10 (Fig. 6K), LAG3 (Fig. 6L), PDCD1 (Fig. 6M), PVR (Fig. 6N), TGFβ1 (Fig. 6O) and TIGIT (Fig. 6P) were greater in the high-risk group, indicating a better immune response.

Drug sensitivity analysis

In addition, we analysed the correlation between the risk score and sensitivity to drugs commonly used for HCC treatment in the clinic. We found that the sensitivity to sorafenib (Supplementary Figure S2A), lapatinib (Supplementary Figure S2B), and erlotinib (Supplementary Figure S2C) was greater in the high-risk group, while the sensitivity to doxorubicin (Supplementary Figure S2D), mitomycin (Supplementary Figure S2E) and gemcitabine (Supplementary Figure S2F) was greater in the low-risk group. The signature showed the potential to guide clinical medication.

The matrix stiffness-related ECM protein DYNLL1 is highly expressed in HCC and is associated with poor prognosis

According to the TCGA data, DYNLL1 was upregulated in tumour tissues (Fig. 7A), similar to our immunohistochemical results (Fig. 7B). Moreover, we found that DYNLL1 was correlated with poor outcomes in HCC patients (Fig. 7C, $p=8.3e-05$). In stages I-III, DYNLL1 expression increased with each stage (Fig. 7D, F=4.75, $p=0.003$). Furthermore, we found that DYNLL1 was correlated with LOX and CO1LA1, indicating that DYNLL1 was associated with mechanism stiffness (Fig. 7E). Single-cell sequencing revealed that DYNLL1 was expressed at relatively low levels in $CD4^+$ T and $CD8^+$ T cells and was highly expressed in T_{reg} cells, fibroblasts, and endothelial cells (Fig. 7F, G, H).

DYNLL1 influences the proliferation, apoptosis, migration and Wnt/β-catenin pathway in HCC

A series of in vitro experiments were conducted to validate the role of DYNLL1 in HCC. To identify the siRNA with the greatest effect on knocking down DYNLL1, we performed qPCR experiments in Huh7 and HepG2 cells, and the si-2 sequence was selected for subsequent experiments (Fig. 8A). We performed a CCK-8 assay and found that knockdown of DYNLL1 significantly reduced the proliferation of HCC cells, indicating that DYNLL1 promoted HCC cell proliferation (Fig. 8B). An apoptosis assay verified that DYNLL1 inhibited HCC cell apoptosis (Fig. 8C). The above results suggest that DYNLL1 promoted the development of HCC by promoting the proliferation of HCC cells and inhibiting their apoptosis. Wound healing assays revealed that knockdown of DYNLL1 decreased the rate of wound healing, suggesting that DYNLL1 promotes cell migration (Fig. 8D). We further investigated whether DYNLL1 affects epithelial–mesenchymal transition (EMT) in HCC cells. We found that knockdown of DYNLL1 increased the expression level of E-cadherin but decreased the expression levels of N-cadherin and vimentin (Fig. 8E). In addition, after the knockdown of DYNLL1, the expression levels of β-catenin, cyclin D1, and c-Myc decreased (Fig. 8F),

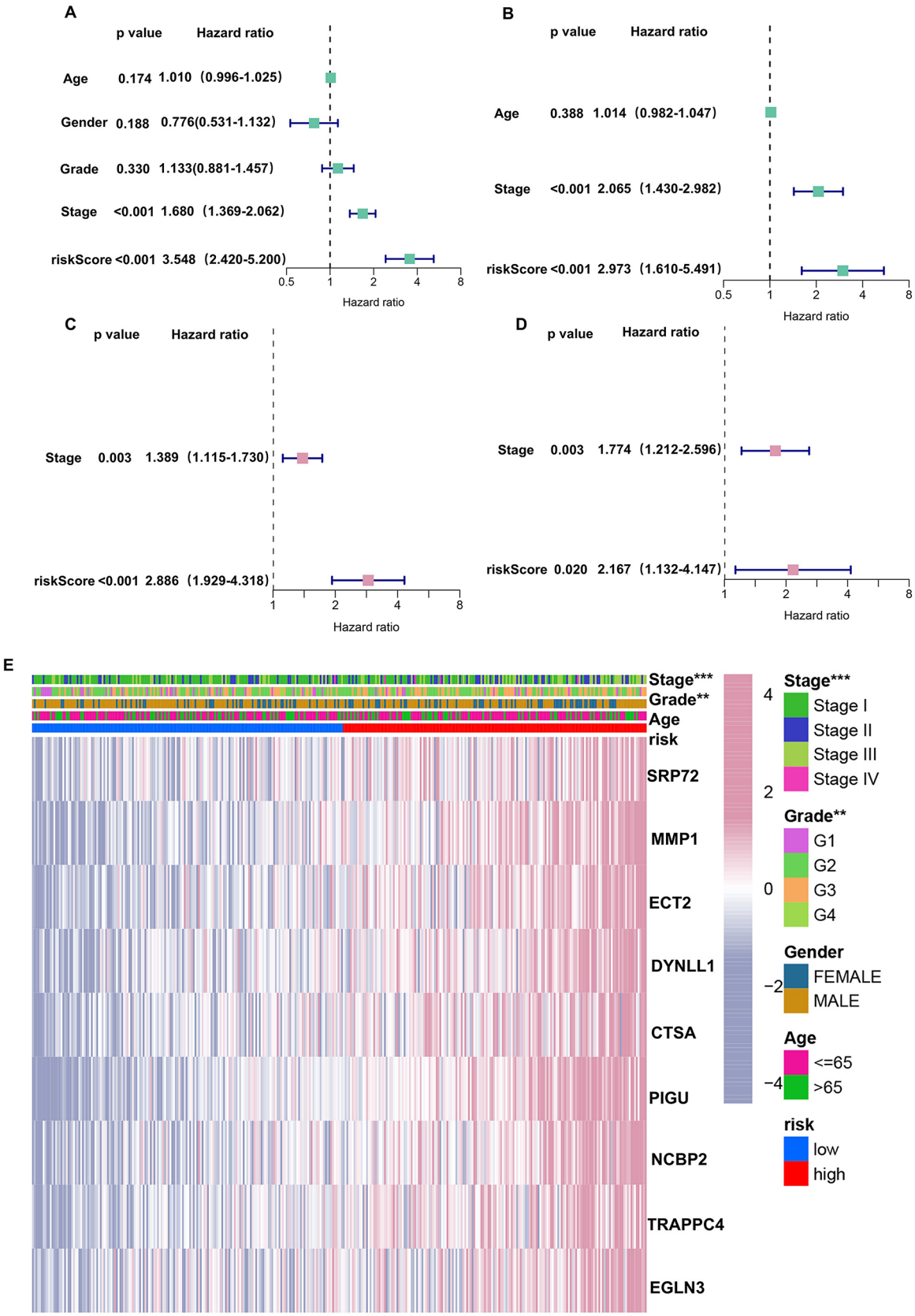

Fig. 4 (See legend on next page.)

(See figure on previous page.)

Fig. 4 Evaluation of the accuracy of the matrix stiffness-related ECM gene prognostic signature in HCC. (**A**-**B**) Forest plot of univariate Cox regression analysis for different clinical factors and risk scores in the TCGA and ICGC cohorts. (**C**-**D**) Forest plot of multivariate Cox regression analysis for different clinical factors and risk scores in the TCGA and ICGC cohorts. (**E**) Distribution heatmap of 9 predictive matrix stiffness-related ECM genes and clinicopathological variables in the high- and low-risk groups. *$P < 0.05$, **$P < 0.01$, ***$P < 0.001$, ****$P < 0.001$; ns, not significant

revealing that DYNLL1 influences the Wnt/β-catenin pathway.

DYNLL1 influences the progression of HCC through the Wnt/β-catenin signalling pathway

To further investigate whether DYNLL1 promotes HCC progression through the Wnt/β-catenin pathway, we treated the HCC cell lines with 20 mM LiCl (an activator of the Wnt/β-catenin pathway) after transfecting them with si-DYNLL1. CCK-8 assay showed that the inhibitory effect on HCC cell proliferation after DYNLL1 knockdown was reversed by LiCl (Fig. 9A). Meanwhile, the Wound-healing assay and apoptosis assay showed that the inhibitory effect of DYNLL1 knockdown on HCC cell migration and the promotion of apoptosis were also reversed by LiCl (Fig. 9B, C). Moreover, the Wnt/β-catenin pathway protein expressions were all upregulated after being treated with LiCl in the si-DYNLL1 group, while in the control group, the expression of these proteins wasn't changed (Fig. 9D). All of these above indicate that DYNLL1 may promote proliferation, and migration, and inhibit the apoptosis of HCC cells through the Wnt/β-catenin pathway.

DYNLL1 promotes HCC progression in vivo

A xenograft tumour model was used to further investigate the role of DYNLL1 in HCC progression. Huh7 cells with stable knockdown of DYNLL1 were inoculated subcutaneously into nude mice. The tumour volumes and weights in the DYNLL1 knockdown group were lower than in the control group (Fig. 10A, B, C). The percentage of Ki-67 was also reduced as shown in the DYNLL1 knockdown group (Fig. 10D). This indicated that the tumour growth was inhibited after the knockdown of DYNLL1. Moreover, the IHC staining revealed that the expression of E-cadherin was higher in the DYNLL1 knockdown group, while N-cadherin and vimentin were lower (Fig. 10E). This preliminarily indicated the knockdown of DYNLL1 may inhibit the EMT of HCC. In addition, the expression of the Wnt/β-catenin pathway proteins was all downregulated after the DYNLL1 knockdown (Fig. 10F), indicating that DYNLL1 may promote HCC progression through the Wnt/β-catenin pathway.

Discussion

In this study, we identified 65 matrix stiffness-related ECM DEGs from the TCGA database based on a systematic analysis. KEGG analysis confirmed that these genes were correlated with the notch signalling pathway, the cell cycle, the PPAR signalling pathway, chemokine signalling pathways, the TGF-beta signalling pathway, and the HIF-1 signalling pathway. Then, we constructed a novel prognostic signature through Lasso regression analysis and identified 9 genes: MMP1, ECT2, DYNLL1, NCBP2, CTSA, PIGU, TRAPPC4, EGLN3, and SRP72. Subsequently, the prognostic value of the 9-gene signature was validated by the TCGA and ICGC databases. We divided HCC patients into high- and low-risk groups based on the median risk score. The results of the ROC curve, Kaplan–Meier curve, and nomogram analyses revealed that the prognostic signature performed well in predicting the prognosis of HCC patients. More importantly, univariate and multivariate independent prognostic analyses validated the independent prognostic value of the gene signature. Furthermore, PCA and t-SNE maps were used to visualize the ability of the prognostic signature to stratify HCC patients. Functional analysis revealed that the DEGs were enriched in immune response and tumour-related pathways. We found that immune cell infiltration and the expression of immune checkpoints in the high-risk group were greater than those in the low-risk group. In addition, the signature showed the potential to guide chemotherapy options in the clinic. Patients with different risk scores have different drug sensitivities. Finally, we performed in vitro and in vivo experiments to validate that DYNLL1 was upregulated in HCC and promoted the development of HCC by promoting proliferation, migration, and inhibiting the apoptosis of HCC cells through the Wnt/β-catenin pathway. These results indicated that DYNLL1 has excellent potential as a biomarker for HCC.

Cirrhosis is the final stage of chronic liver disease and a common precursor to HCC. This process involves the activation of hepatic stellate cells (HSCs), the secretion of collagen to activate the Hippo effector TAZ, and an increase in liver tissue matrix stiffness, which creates a microenvironment that is prone to tumour development [30]. Several studies have demonstrated the importance of matrix stiffness-related proteins in cancer biology, which could be potential targets for cancer therapy [7, 31, 32]. For example, HSCs bind endostatin peptides released by cathepsin S via integrin α5β1 signalling, resulting in increased matrix stiffness [33]. TGF-β1 induces the expression of LOX in cancer, which leads to increased matrix stiffness and suppression of the immune response, thereby promoting tumourigenesis [34, 35]. Additionally, increased matrix stiffness promotes the differentiation of HSCs into tumour-associated fibroblasts (CAFs), leading

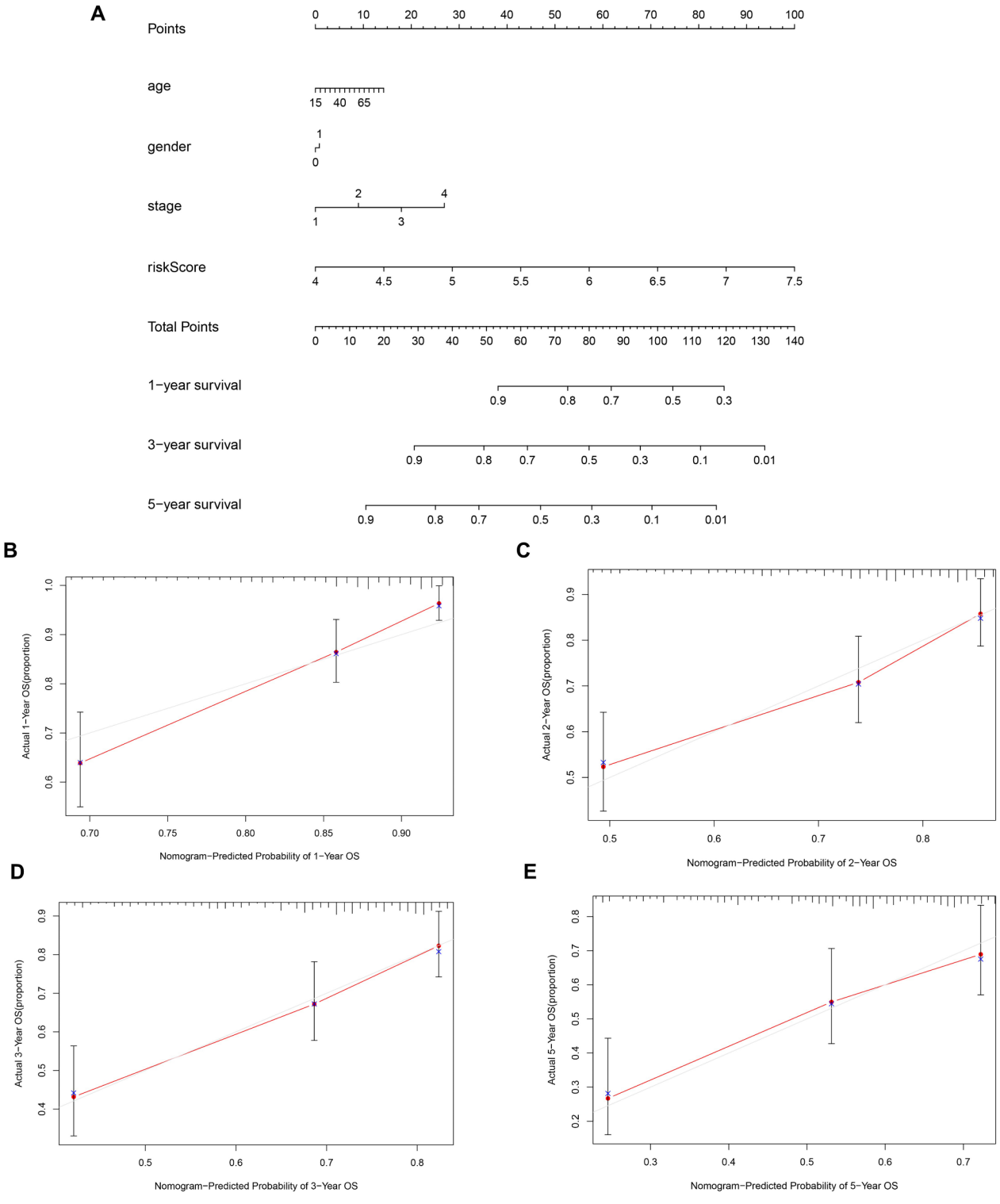

Fig. 5 Construction and verification of the predictive nomogram. (**A**) A nomogram considering clinicopathological factors and risk scores for predicting the 1-year, 3-year, and 5-year overall survival rates of patients with HCC. (**B**-**E**) The calibration curve for evaluating the accuracy of the nomogram model

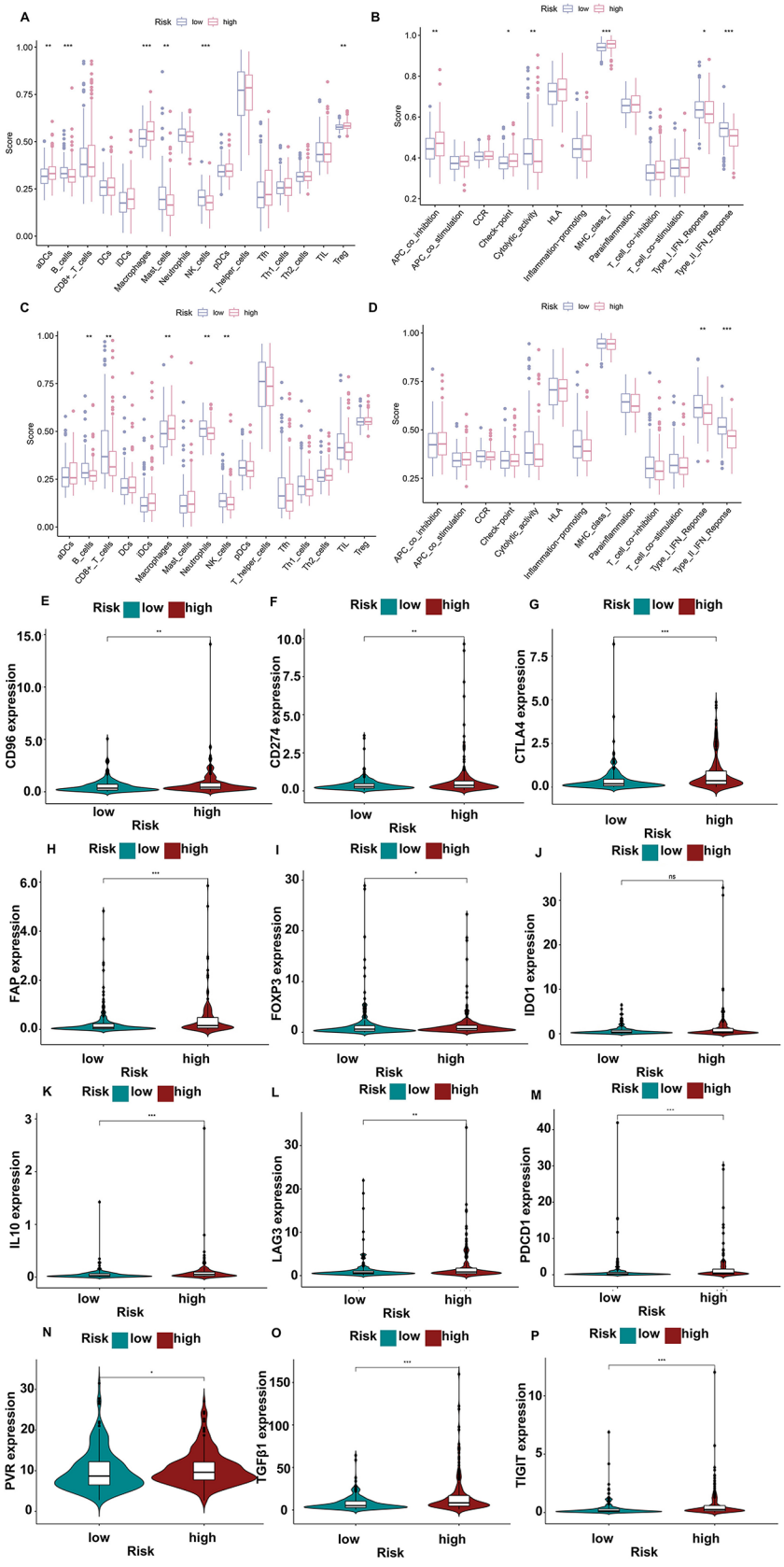

Fig. 6 (See legend on next page.)

(See figure on previous page.)

Fig. 6 Analysis of the immune infiltration landscape and immune checkpoints in HCC patients. (**A**-**B**) The distribution of tumour-infiltrating immune cells between the high- and low-risk groups based on the matrix stiffness-related ECM gene signature. (**C**-**D**) Comparison of box plots of 13 immune functions in the high- and low-risk groups of HCC patients. (**E**-**P**) Comparison of immune checkpoint genes between the high- and low-risk groups. *$P < 0.05$, **$P < 0.01$, ***$P < 0.001$, ****$P < 0.001$; ns, not significant

to a vicious cycle [36]. Investigating the precise function of matrix stiffness-related proteins in cancer has become a major focus of contemporary cancer treatment.

DYNLL1 has multiple mechanisms of action in tumours. It has been shown to inhibit DNA end resection in BRCA1-deficient ovarian cancer by binding to MRE11, which increases chemotherapy resistance [15]. Berkel C. et al. [37] reported that DYNLL1 was highly expressed in HCC patients and was associated with shorter OS and PFS. However, the conclusions are limited by the fact that the article only presented the results of the data analysis and lacked experimental evidence. DYNLL1 also plays a critical role in negatively regulating apoptosis. For instance, DLEU1 upregulates DYNLL1 to inhibit apoptosis in oesophageal squamous carcinoma cells [38]. In immature B cells, DYNLL1 has a negative regulatory effect on the proapoptotic activity of Bim [39]. Deletion of DYNLL1 inhibited the occurrence and expansion of MYC-driven B-cell lymphomas in mice [40]. This finding suggests that DYNLL1 may play a critical role in the immune response of tumour cells and the promotion of cancer cell survival. Our study expands the mechanism of DYNLL1 in HCC though both in vitro and in vivo experiments and offers a potential new target for the clinical treatment of HCC patients.

Previous studies have constructed prognostic models and developed biomarkers for cancers [41, 42]. The risk scores of the model constructed in our study can effectively predict the prognosis of patients with HCC. Moreover, all nine genes encoded matrix stiffness-related ECM proteins, which have not been previously reported in related models. We revealed the relationship between matrix stiffness-related ECM proteins and immunity, as well as drug resistance. This provides preliminary evidence for the assessment of the efficacy of immunotherapy and chemotherapy treatments in clinical practice. Using in vitro and in vivo experiments, our study preliminarily investigated the effects of DYNLL1 on the proliferation, migration, and apoptosis of HCC cells and the possible pathways affected by DYNLL1, which may provide potential targets for the treatment of HCC. However, our study also has several limitations. All data analyses were based on databases rather than realistic case cohorts, and further large clinical trials are needed to verify the accuracy of these signatures. Second, our study on DYNLL1 included only in vitro and in vivo experiments, and further studies, including clinical trials, are needed if this target is to be used in clinical therapy. Finally, our studies on matrix stiffness-associated ECM proteins in the TME are insufficient, and these studies need to be further expanded upon.

In summary, we identified matrix stiffness-related ECM proteins as independent predictors of HCC prognosis and highlighted their significance in the occurrence and progression of HCC. We validated the molecular mechanism by which DYNLL1, an ECM protein related to matrix stiffness, promotes HCC progression based on bioinformatics results. These results indicate that DYNLL1 is a potential target for HCC treatment and may also play an important role in the TME.

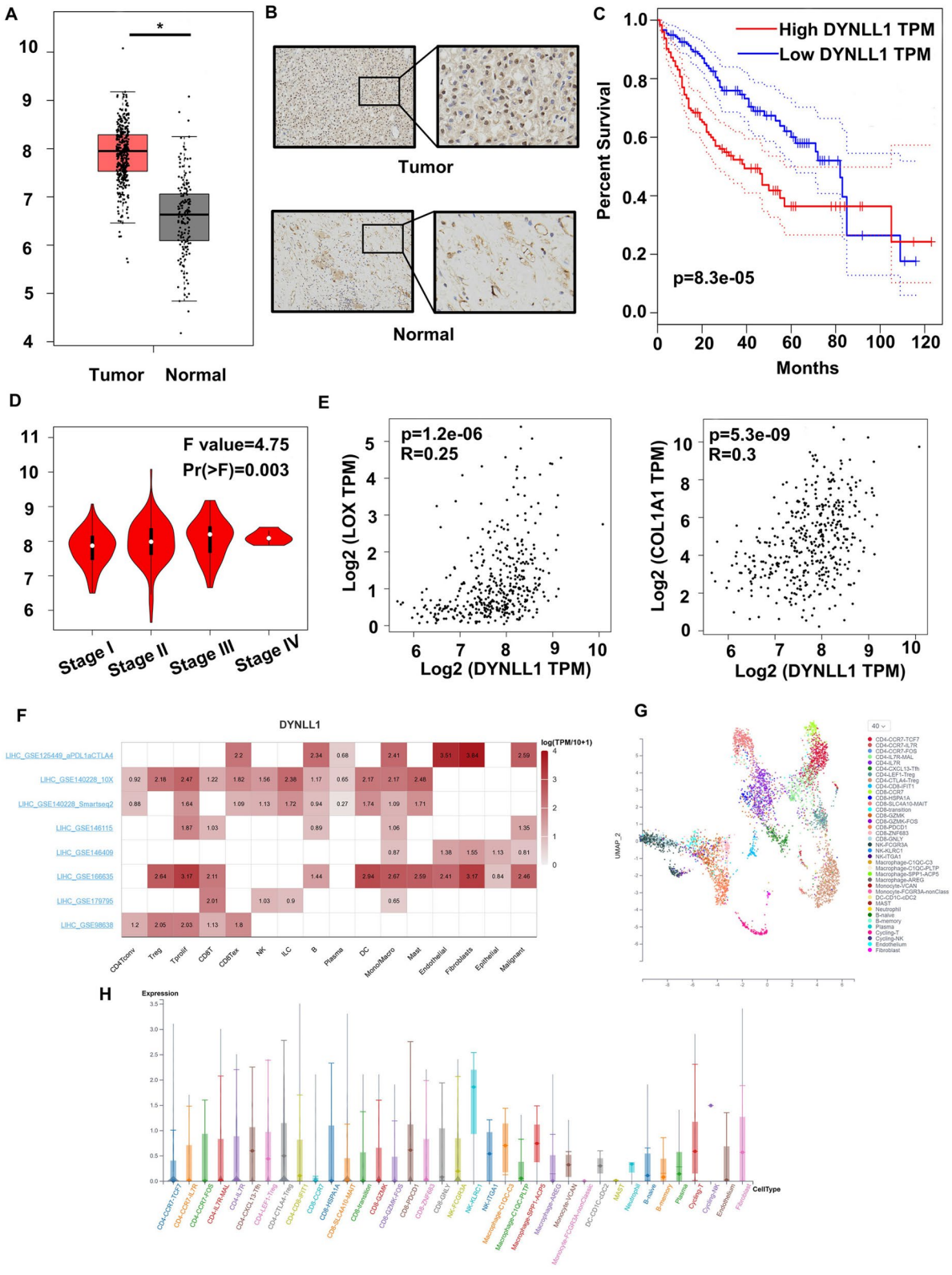

Fig. 7 Matrix stiffness-related ECM protein DYNLL1 in HCC. (**A**) The expression of DYNLL1 in HCC and normal tissues in TCGA. (**B**) IHC staining of DYNLL1 in HCC and normal tissues. (**C**) Survival curve of HCC patients in TCGA stratified by DYNLL1 expression. (**D**) Association of DYNLL1 expression with different stages of HCC. (**E**) Correlation of DYNLL1 with the matrix stiffness-related proteins LOX and CO1LA1. (**F**) UMAP of different immune cells in HCC from the scTIME website. (**G**-**H**) Expression of DYNLL1 in different immune cells according to the TISCH2 and scTIME databases

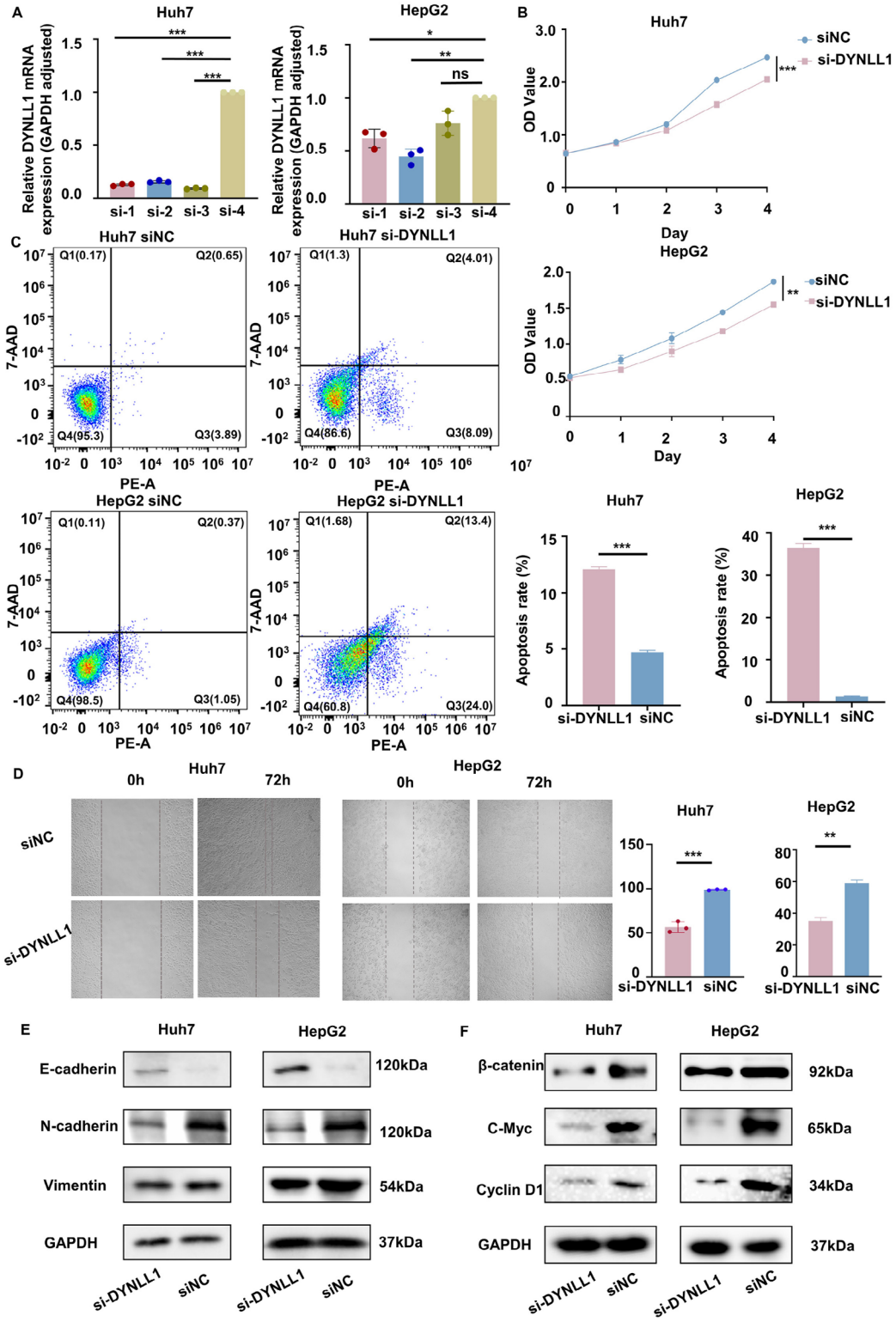

Fig. 8 The influence of DYNLL1 on proliferation, apoptosis, migration and Wnt/β-catenin signalling pathway in HCC. (**A**) PCR was used to validate DYNLL1 knockdown in Huh7 and HepG2 cells. Pink represents si-1, blue represents si-2, dark green represents si-3, and light green represents si-4 group. (**B**) CCK-8 proliferation assays in Huh7 and HepG2 cell lines after DYNLL1 knockdown. (**C**) Apoptosis assay in Huh7 and HepG2 cell lines after DYNLL1 knockdown. (**D**) Wound healing assays in Huh7 and HepG2 cell lines after DYNLL1 knockdown. (**E**) Western blotting revealed changes in the expression levels of EMT-related proteins in HCC cells. (**F**) Western blotting revealed changes in the expression levels of proteins in the Wnt/β-catenin pathway. Pink represents si-DYNLL1,, and blue represents the siNC group. All the data are expressed as the mean ± SD. *$P < 0.05$, **$P < 0.01$, ***$P < 0.001$, ****$P < 0.001$; ns, not significant

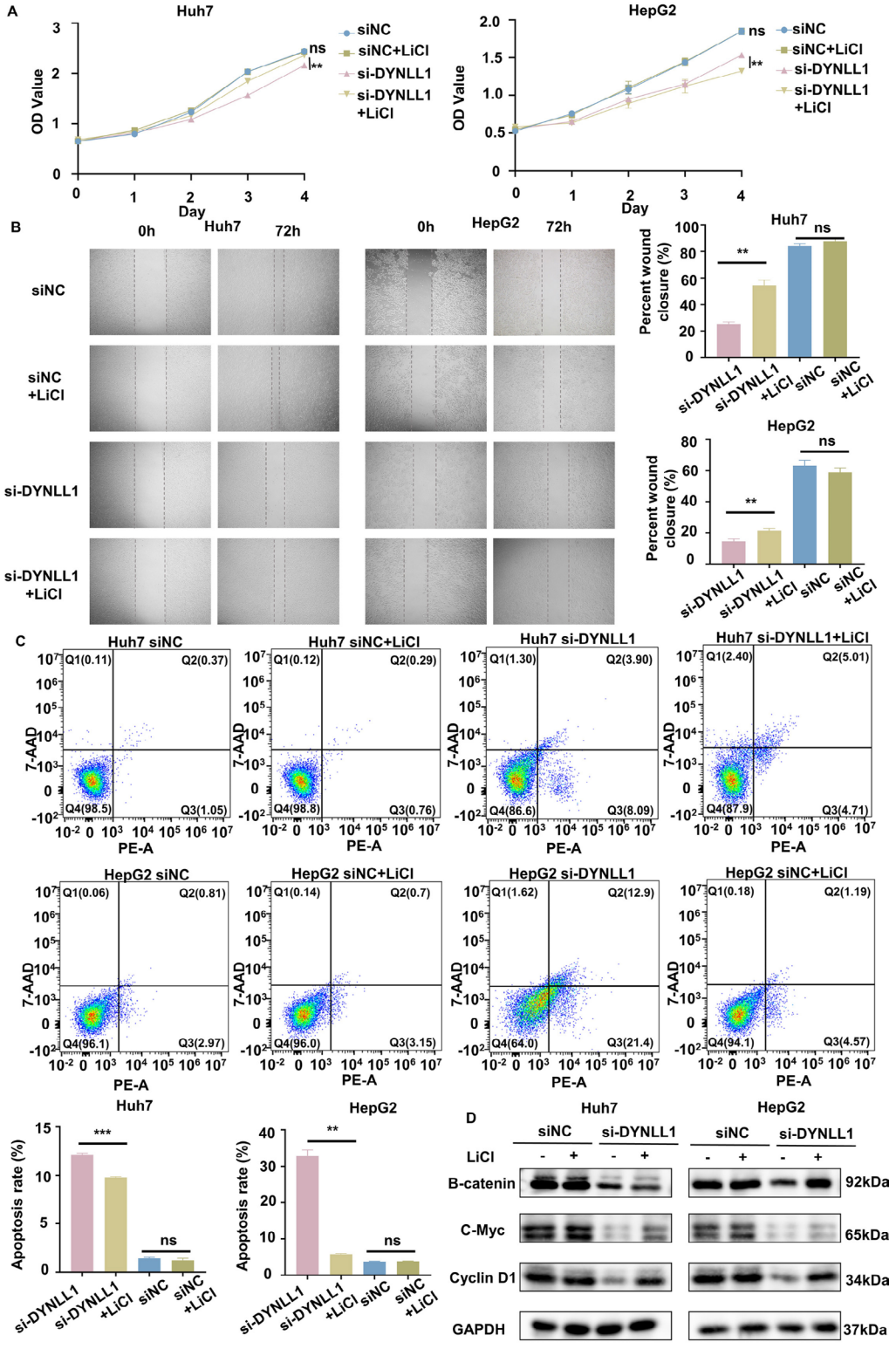

Fig. 9 DYNLL1 affects the progression of HCC through the Wnt/β-catenin pathway. (**A**) CCK-8 assays in Huh7 and HepG2 cell lines treated with LiCl after knockdown of DYNLL1. (**B**) Wound healing assays in Huh7 and HepG2 cell lines treated with LiCl after knockdown of DYNLL1. (**C**) Apoptosis assays in Huh7 and HepG2 cell lines treated with LiCl after knockdown of DYNLL1. (**D**) Western blotting revealed changes in the expression levels of proteins in the Wnt/β-catenin pathway from Huh7 and HepG2 cell lines treated with LiCl after the knockdown of DYNLL1. Pink represents si-DYNLL1, blue represents siNC, dark green represents siNC + LiCl, and light green represents si-DYNLL1 + LiCl group. All the data are expressed as the mean ± SD. *$P < 0.05$, **$P < 0.01$, ***$P < 0.001$, ****$P < 0.001$; ns, not significant

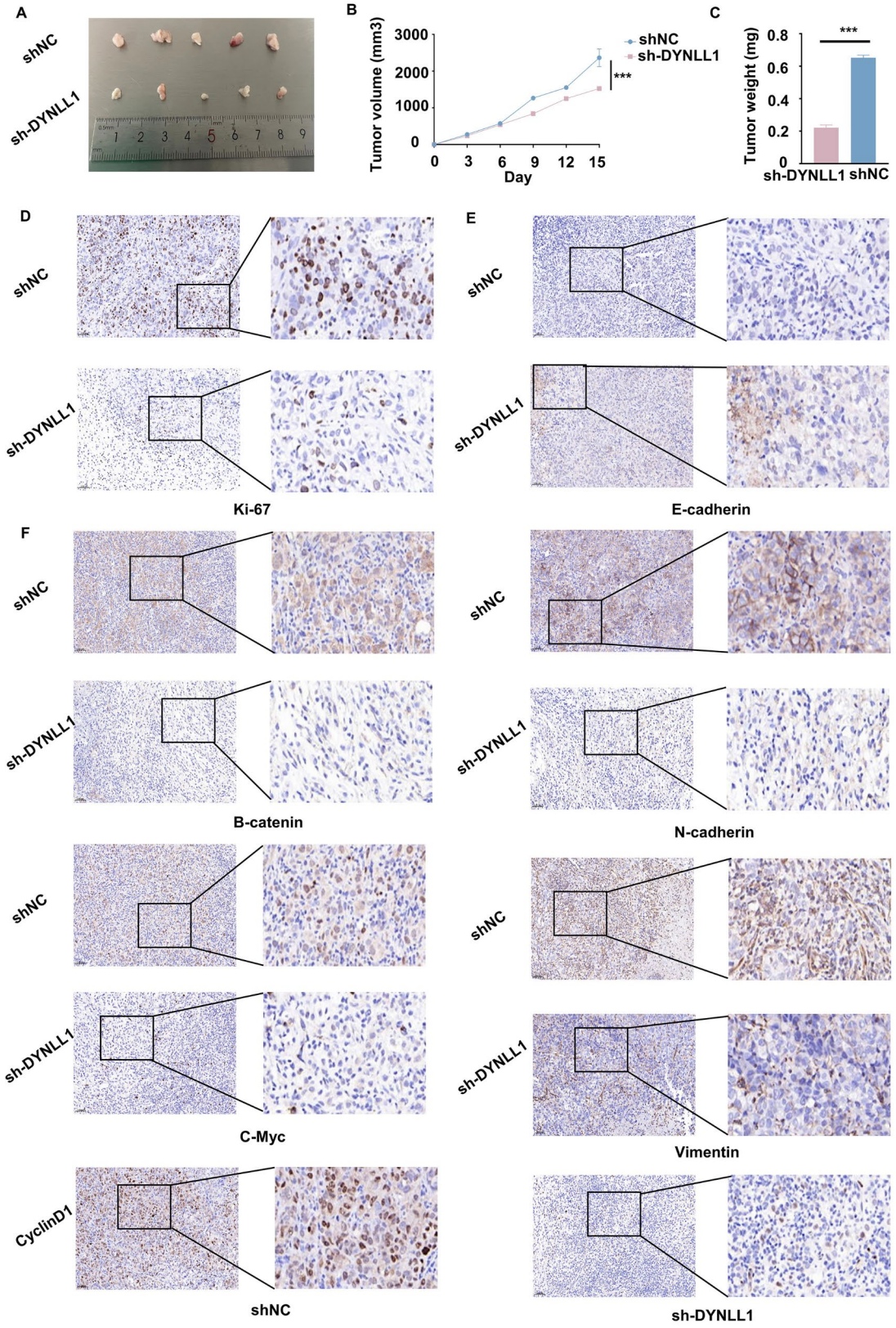

Fig. 10 DYNLL1 promotes HCC progression in vivo. (**A**-**C**) The growth volume and weight of the xenograft tumour. (**D**) Representative Ki-67 IHC staining of tumours. (**E**) Representative E-cadherin, N-cadherin, and vimentin IHC staining of tumours. (**F**) Representative Cyclin D1, β-catenin, and c-Myc IHC staining of tumours. Pink represents xenograft tumours from stable DYNLL1 knockdown huh7 cells, blue represents xenograft tumours from control huh7 cells. All the data are expressed as the mean ± SD. *$P < 0.05$, **$P < 0.01$, ***$P < 0.001$, ****$P < 0.001$; ns, not significant

Conclusion

Matrix stiffness-related ECM proteins could be independent predictors of HCC prognosis. DYNLL1, an oncogenic gene in HCC, has the potential to be a new target for HCC treatment.

Supplementary Information

The online version contains supplementary material available at https://doi.org/10.1186/s12885-024-12973-5.

Supplementary Material 1

Acknowledgements
Not applicable.

Author contributions
Conceptualization, Y.S., J.C. and Z.Z.; methodology, J.W. and X.H.; software, Y.X.; validation, Y.S., J.C. and Z.Z.; formal analysis, J.L. and L.W.; investigation, S.Y. and S.W.; resources, X.H.; data curation, Z.Z.; writing—original draft preparation, Y.S., J.C. and Z.Z.; writing—review and editing, Y.S., J.C. and Z.Z.; visualization, Y.S., S.Y. and S.W.; supervision, L.F. and X.X.; funding acquisition, X.X. All authors have read and agreed to the published version of the manuscript.

Funding
This research was funded by the National Natural Science Foundation of China, grant number 31971166.

Data availability
The datasets used and/or analyzed during the current study are available from the corresponding author upon reasonable request.

Declarations

Ethics approval and consent to participate
The study was approved by the Ethics Committee of Renmin Hospital of Wuhan University (WDRY2023-K030). All participants in the study were anonymous, and the study did not involve patient privacy. The Ethics Committee approved the informed consent exemption for this study. The study related to animals was approved by the Ethics Committee of Renmin Hospital of Wuhan University (202300384) on Jan 1, 2024.

Consent for publication
Not applicable.

Competing interests
The authors declare no competing interests.

Author details
[1]Cancer Center, Renmin Hospital of Wuhan University, Wuhan 430060, China

Received: 3 May 2024 / Accepted: 20 September 2024
Published online: 30 September 2024

References

1. Llovet JM, Kelley RK, Villanueva A, Singal AG, Pikarsky E, Roayaie S, Lencioni R, Koike K, Zucman-Rossi J, Finn RS. Hepatocellular carcinoma. Nat Rev Dis Primers. 2021;7(1):6.
2. Zhu P, Liao W, Zhang WG, Chen L, Shu C, Zhang ZW, Huang ZY, Chen YF, Lau WY, Zhang BX, et al. A prospective study using propensity score matching to compare long-term survival outcomes after Robotic-assisted, laparoscopic, or Open Liver Resection for patients with BCLC stage 0-A Hepatocellular Carcinoma. Ann Surg. 2023;277(1):e103–11.
3. Huang J, Zhang L, Wan D, Zhou L, Zheng S, Lin S, Qiao Y. Extracellular matrix and its therapeutic potential for cancer treatment. Signal Transduct Target Ther. 2021;6(1):153.
4. Dong Y, Zheng Q, Wang Z, Lin X, You Y, Wu S, Wang Y, Hu C, Xie X, Chen J, et al. Higher matrix stiffness as an independent initiator triggers epithelial-mesenchymal transition and facilitates HCC metastasis. J Hematol Oncol. 2019;12(1):112.
5. Wu B, Liu DA, Guan L, Myint PK, Chin L, Dang H, Xu Y, Ren J, Li T, Yu Z, et al. Stiff matrix induces exosome secretion to promote tumour growth. Nat Cell Biol. 2023;25(3):415–24.
6. Li N, Zhang X, Zhou J, Li W, Shu X, Wu Y, Long M. Multiscale biomechanics and mechanotransduction from liver fibrosis to cancer. Adv Drug Deliv Rev. 2022;188:114448.
7. Lachowski D, Matellan C, Gopal S, Cortes E, Robinson BK, Saiani A, Miller AF, Stevens MM. Del Río Hernández AE: substrate stiffness-driven membrane tension modulates vesicular trafficking via Caveolin-1. ACS Nano. 2022;16(3):4322–37.
8. Nicolas-Boluda A, Vaquero J, Vimeux L, Guilbert T, Barrin S, Kantari-Mimoun C, Ponzo M, Renault G, Deptula P, Pogoda K et al. Tumour stiffening reversion through collagen crosslinking inhibition improves T cell migration and anti-PD-1 treatment. Elife 2021, 10.
9. Zhu Y, Yang J, Xu D, Gao XM, Zhang Z, Hsu JL, Li CW, Lim SO, Sheng YY, Zhang Y, et al. Disruption of tumour-associated macrophage trafficking by the osteopontin-induced colony-stimulating factor-1 signalling sensitises hepatocellular carcinoma to anti-PD-L1 blockade. Gut. 2019;68(9):1653–66.
10. Yang Z, Zhou L, Si T, Chen S, Liu C, Ng KK, Wang Z, Chen Z, Qiu C, Liu G, et al. Lysyl hydroxylase LH1 promotes confined migration and metastasis of cancer cells by stabilizing Septin2 to enhance actin network. Mol Cancer. 2023;22(1):21.
11. Yang K, Xie Y, Xue L, Li F, Luo C, Liang W, Zhang H, Li Y, Ren Y, Zhao M, et al. M2 tumour-associated macrophage mediates the maintenance of stemness to promote cisplatin resistance by secreting TGF-β1 in esophageal squamous cell carcinoma. J Translational Med. 2023;21(1):26.
12. Chen Z, Li H, Li Z, Chen S, Huang X, Zheng Z, Qian X, Zhang L, Long G, Xie J, et al. SHH/GLI2-TGF-β1 feedback loop between cancer cells and tumour-associated macrophages maintains epithelial-mesenchymal transition and endoplasmic reticulum homeostasis in cholangiocarcinoma. Pharmacol Res. 2023;187:106564.
13. Swift ML, Zhou R, Syed A, Moreau LA, Tomasik B, Tainer JA, Konstantinopoulos PA, D'Andrea AD, He YJ, Chowdhury D. Dynamics of the DYNLL1-MRE11 complex regulate DNA end resection and recruitment of Shieldin to DSBs. Nat Struct Mol Biol. 2023;30(10):1456–67.
14. Becker JR, Cuella-Martin R, Barazas M, Liu R, Oliveira C, Oliver AW, Bilham K, Holt AB, Blackford AN, Heierhorst J, et al. The ASCIZ-DYNLL1 axis promotes 53BP1-dependent non-homologous end joining and PARP inhibitor sensitivity. Nat Commun. 2018;9(1):5406.
15. Sun X, Meng F, Nong M, Fang H, Lu C, Wang Y, Zhang P. Single-cell dissection reveals the role of aggrephagy patterns in tumour microenvironment components aiding predicting prognosis and immunotherapy on lung adenocarcinoma. Aging. 2023;15(23):14333–71.
16. He YJ, Meghani K, Caron MC, Yang C, Ronato DA, Bian J, Sharma A, Moore J, Niraj J, Detappe A, et al. DYNLL1 binds to MRE11 to limit DNA end resection in BRCA1-deficient cells. Nature. 2018;563(7732):522–6.
17. Syed A, Tainer JA. The MRE11-RAD50-NBS1 Complex conducts the Orchestration of damage signaling and outcomes to stress in DNA replication and repair. Annu Rev Biochem. 2018;87:263–94.
18. Shibata A, Moiani D, Arvai AS, Perry J, Harding SM, Genois MM, Maity R, van Rossum-Fikkert S, Kertokalio A, Romoli F, et al. DNA double-strand break repair pathway choice is directed by distinct MRE11 nuclease activities. Mol Cell. 2014;53(1):7–18.
19. Berkel C, Cacan E. Involvement of ATMIN-DYNLL1-MRN axis in the progression and aggressiveness of serous ovarian cancer. Biochem Biophys Res Commun. 2021;570:74–81.
20. Liu Y, Li Z, Zhang J, Liu W, Guan S, Zhan Y, Fang Y, Li Y, Deng H, Shen Z. DYNLL1 accelerates cell cycle via ILF2/CDK4 axis to promote hepatocellular carcinoma development and palbociclib sensitivity. Br J Cancer. 2024;131(2):243–57.
21. Ritchie ME, Phipson B, Wu D, Hu Y, Law CW, Shi W, Smyth GK. Limma powers differential expression analyses for RNA-sequencing and microarray studies. Nucleic Acids Res. 2015;43(7):e47.

22. Wu T, Hu E, Xu S, Chen M, Guo P, Dai Z, Feng T, Zhou L, Tang W, Zhan L, et al. clusterProfiler 4.0: a universal enrichment tool for interpreting omics data. Innov (Camb). 2021;2(3):100141.
23. Mayakonda A, Lin DC, Assenov Y, Plass C, Koeffler HP. Maftools: efficient and comprehensive analysis of somatic variants in cancer. Genome Res. 2018;28(11):1747–56.
24. Hänzelmann S, Castelo R, Guinney J. GSVA: gene set variation analysis for microarray and RNA-seq data. BMC Bioinformatics. 2013;14:7.
25. Morgan MFS, Gentleman R. GSEABase: Gene set enrichment data structures and methods_. R package version 1.60.0. 2022.
26. Maeser D, Gruener RF, Huang RS. oncoPredict: an R package for predicting in vivo or cancer patient drug response and biomarkers from cell line screening data. Brief Bioinform 2021, 22(6).
27. R Core Team. (2022). R: A language and environment for statistical computing. R Foundation for Statistical Computing, Vienna, Austria. URL https://www.R-project.org/
28. Wu S, Zheng Q, Xing X, Dong Y, Wang Y, You Y, Chen R, Hu C, Chen J, Gao D, et al. Matrix stiffness-upregulated LOXL2 promotes fibronectin production, MMP9 and CXCL12 expression and BMDCs recruitment to assist pre-metastatic niche formation. J Experimental Clin cancer Research: CR. 2018;37(1):99.
29. Xu S, Xu H, Wang W, Li S, Li H, Li T, Zhang W, Yu X, Liu L. The role of collagen in cancer: from bench to bedside. J Translational Med. 2019;17(1):309.
30. Filliol A, Saito Y, Nair A, Dapito DH, Yu LX, Ravichandra A, Bhattacharjee S, Affo S, Fujiwara N, Su H, et al. Opposing roles of hepatic stellate cell subpopulations in hepatocarcinogenesis. Nature. 2022;610(7931):356–65.
31. Cai J, Chen T, Jiang Z, Yan J, Ye Z, Ruan Y, Tao L, Shen Z, Liang X, Wang Y, et al. Bulk and single-cell transcriptome profiling reveal extracellular matrix mechanical regulation of lipid metabolism reprograming through YAP/TEAD4/ACADL axis in hepatocellular carcinoma. Int J Biol Sci. 2023;19(7):2114–31.
32. Zhao W, Yang A, Chen W, Wang P, Liu T, Cong M, Xu A, Yan X, Jia J, You H. Inhibition of lysyl oxidase-like 1 (LOXL1) expression arrests liver fibrosis progression in cirrhosis by reducing elastin crosslinking. Biochim Biophys Acta Mol Basis Dis. 2018;1864(4 Pt A):1129–37.
33. Zuo T, Xie Q, Liu J, Yang J, Shi J, Kong D, Wang Y, Zhang Z, Gao H, Zeng DB, et al. Macrophage-derived cathepsin S remodels the Extracellular Matrix to Promote Liver Fibrogenesis. Gastroenterology. 2023;165(3):746–e761716.
34. Wu S, Xing X, Wang Y, Zhang X, Li M, Wang M, Wang Z, Chen J, Gao D, Zhao Y, et al. The pathological significance of LOXL2 in pre-metastatic niche formation of HCC and its related molecular mechanism. Eur J Cancer. 2021;147:63–73.
35. Wong CC, Tse AP, Huang YP, Zhu YT, Chiu DK, Lai RK, Au SL, Kai AK, Lee JM, Wei LL, et al. Lysyl oxidase-like 2 is critical to tumour microenvironment and metastatic niche formation in hepatocellular carcinoma. Hepatology. 2014;60(5):1645–58.
36. Chen G, Deng Y, Xia B, Lv Y. In situ regulation and mechanisms of 3D matrix stiffness on the activation and reversion of hepatic stellate cells. Adv Healthc Mater. 2023;12(9):e2202560.
37. Berkel C, Cacan E. DYNLL1 is hypomethylated and upregulated in a tumour stage- and grade-dependent manner and associated with increased mortality in hepatocellular carcinoma. Exp Mol Pathol. 2020;117:104567.
38. Li Q, Zhang Z, Jiang H, Hou J, Chai Y, Nan H, Li F, Wang L. DLEU1 promotes cell survival by preventing DYNLL1 degradation in esophageal squamous cell carcinoma. J Translational Med. 2022;20(1):245.
39. Jurado S, Gleeson K, O'Donnell K, Izon DJ, Walkley CR, Strasser A, Tarlinton DM, Heierhorst J. The zinc-finger protein ASCIZ regulates B cell development via DYNLL1 and bim. J Exp Med. 2012;209(9):1629–39.
40. Wong DM, Li L, Jurado S, King A, Bamford R, Wall M, Walia MK, Kelly GL, Walkley CR, Tarlinton DM, et al. The transcription factor ASCIZ and its target DYNLL1 are essential for the development and expansion of MYC-Driven B cell lymphoma. Cell Rep. 2016;14(6):1488–99.
41. Bian G, Cao J, Li W, Huang D, Ding X, Zang X, Ye Y, Li P. Identification and validation of a Cancer-Testis Antigen-related signature to predict the prognosis in stomach adenocarcinoma. J Cancer. 2024;15(11):3596–611.
42. Gui Z, Ye Y, Li Y, Ren Z, Wei N, Liu L, Wang H, Zhang M. Construction of a novel cancer-associated fibroblast-related signature to predict clinical outcome and immune response in cervical cancer. Transl Oncol. 2024;46:102001.

Publisher's note